THE STRUCTURAL DESIGN OF TALL BUILDINGS
Struct. Design Tall Build. **9**, 251–277 (2000)

ASSESSMENT OF INELASTIC RESPONSE OF BUILDINGS USING FORCE- AND DISPLACEMENT-BASED APPROACHES

B. BORZI AND A. S. ELNASHAI*
Department of Civil and Environmental Engineering, Imperial College, London SW7, U.K.

SUMMARY

In recognition of the increasing importance of accurate seismic vulnerability assessment, this paper deals with procedures and the application of inelastic acceleration and displacement spectra in the seismic assessment of buildings. An identification procedure is outlined, whereby an equivalent single degree of freedom (SDOF) system is devised to represent the building. The SDOF system characteristics (stiffness, strength, post-peak force response and ductility) are readily evaluated from observation of the seismic response of buildings and simple mechanics. The characteristics are then tuned using measurements from instrumented buildings. Based on the earthquake scenario and structural response characteristics, appropriate inelastic acceleration and displacement spectra are selected and used to 'predict' the response. Comparison between the measured and predicted responses for the five buildings studied in the paper confirm the feasibility of the procedure and the realism of the results.

1. INTRODUCTION

A well controlled dataset was employed for the definition of attenuation relationships for inelastic constant ductility displacement and acceleration spectra (Borzi *et al.*, 1999; Borzi & Elnashai, 1999, respectively). The purpose of the aforementioned work was to identify the influence of the ground measurement parameters (magnitude, distance and local site condition) and hysteretic behaviour on the inelastic spectra. The employed dataset comprised 364 accelerograms from an extended area including Europe and its vicinity. Inelastic spectra were derived using two models: an elastic perfectly plastic representation and another more complex system having a yield point, a maximum force point and a post-ultimate branch that may represent hardening as well as softening. Finally, average values of the response modification factors of displacement and acceleration spectra (q and η) were evaluated by means of a comparison between elastic and inelastic spectral ordinates. The response modification coefficients for displacement and acceleration proposed in Borzi *et al.* (1999) and Borzi and Elnashai (in press), respectively, may be used to modify the elastic spectral ordinates to obtain the corresponding inelastic ones. Description of the input motion and the hysteretic models follows.

To evaluate whether the hysteretic models employed for the definition of inelastic response spectra are adequate for describing the global behaviour of structures subjected to earthquake loads, applications to four instrumented structures and a full-scale tested building were undertaken. The five examples studied are fully discussed below.

* Correspondence to: A. S. Elnashai, Department of Civil and Environmental Engineering, Imperial College, College Road, London SW7 2BU.

Contract/grant sponsor: ICONS
Contract/grant sponsor: NODISASTR

Received November 1999
Accepted February 2000

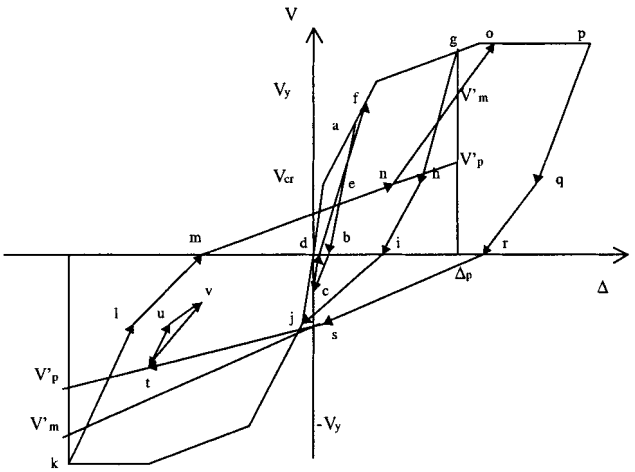

Figure 1. HHS model for structural members

2. INPUT MOTION

The dataset employed for the definition of inelastic constant ductility spectra was assembled by Bommer *et al.* (1998) for the derivation of frequency-dependent attenuation equations for the ordinates of displacement response spectra. All records were filtered individually at Imperial College, London, and used to derive displacement spectra for different levels of damping, from 5 to 30%. The dataset has been adapted from the one employed by Ambraseys *et al.* (1996) to derive attenuation relationships for the ordinates of elastic acceleration response spectra. This is a high quality dataset in terms of both accelerograms that have been individually corrected and information regarding the recording stations and earthquake characteristics.

The accelerograms of the dataset were recorded during 43 earthquakes of magnitude between 5·5 and 7·9, at a distance from the nearest point on the fault of up to 260 km. While the source distance and the surface-wave magnitude are available for all the accelerograms, for three records the local site geology is unknown. For the remaining 180, the percentages of distribution in the three site groupings of rock, stiff and soft soil are 25·0, 51·1 and 23·9%, respectively. For two records, only one component of the motion is available. The total number of records used is 364.

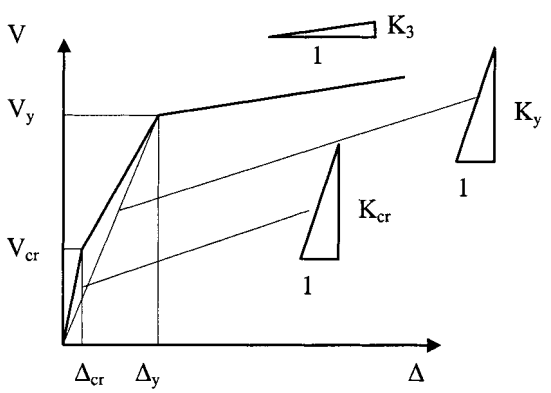

Figure 2. Shape of primary curve used in this work

The attenuation model used in this work is the same as Ambraseys *et al.* (1996) used to define elastic acceleration spectra for Europe. In this attenuation model, three soil types are defined as a function of the shear-wave velocity. When the shear wave exceeds 750 m s^{-1} the soil is classified as rock. A shear-wave velocity less than 360 m s^{-1} leads to categorizing the soil as soft. Stiff soil conditions are assumed in the intermediate range of shear-wave velocity. Further details of the dataset, attenuation relationship and the regression model are given in Bommer and Elnashai (1999).

3. STRUCTURAL MODELS

3.1. Elastic perfectly-plastic model

In order to determine the influence of magnitude, distance and soil condition on inelastic response spectra, attenuation relationships have been defined using an elastic perfectly-plastic response model (EPP). The EPP model was employed since it is the simplest form of inelastic force-resistance as well as being the basis for early relationships between seismic motion and response modification factors. Moreover, by virtue of its two parameters definition: level of force-resistance and stiffness. Few structural characteristics are included; hence the influence of strong-motion records may be better visualized. The stiffness of the inelastic spring corresponds to the period of vibration for which the spectral ordinate has to be calculated and the resistance is derived iteratively. In this work, inelastic constant ductility spectra were obtained. Therefore the resistance of the system corresponds to a required ductility equal to the target ductility. The ensuing inelastic spectra would reflect solely the characteristics of the input motion.

3.2. Hysteretic hardening–softening model

The influence of hysteretic behaviour on inelastic response spectra is studied by employing a hysteretic hardening–softening model (HHS). The structural model is characterized by the definition of a primary curve and unloading and reloading rules. The primary curve for a hysteretic force–displacement relationship is defined as the envelope curve under cyclic loads. For non-degrading models the primary curve is considered as the response curve under monotonic load. In this model the primary curve is used to define the limits for member strength. On the primary curve two points have to be defined as cracking and yielding loads (V_{cr} and V_y) and the corresponding displacements (Δ_{cr} and Δ_y) as shown in Figure 1. If, for example, this model were used to describe the hysteretic behaviour of reinforced concrete members, the cracking load would correspond to the spread of cracks in the concrete and the yielding load would be the load at which the strain in bars in equal to the yield strain of steel. Unloading and reloading branches of the HHS model have been established through a statistical analysis of experimental data. A comprehensive experimental investigation was conducted for this purpose (Saatcioglu *et al.*, 1988; Saatcioglu and Ozcebe, 1989).

The input parameters for the HHS model described above are the monotonic curve and the relationship between axial compressive force and nominal concentric axial capacity. In order to define the inelastic constant ductility spectra the magnitude of the monotonic curve is not an input parameter. It is defined in an iterative way forcing the relationship between maximum and yield displacements to satisfy the target ductility. To obtain the inelastic spectra, an approximation of the primary curve with three linear branches has been assumed (Figure 2). Consequently, the input parameters defining the shape of the primary curve are:

(1) the relationship between the cracking and the yielding load (V_{cr}/V_y);
(2) the relationship between the stiffness before the cracking load and the secant stiffness (K_{cr}/K_y);
(3) the slope of the post yield branch.

Table 1. Main shock magnitudes

Magnitude Scale	Value	Source
Local (M_L)	6·4	TERRAscope (Kanamori)
Surface (M_S)	6·8	NEIC
Moment (M_W)	6·7	Kanamori (EERI, 1994)

To select the values of parameters to be employed, an analysis of the influence of each parameter on the inelastic spectra was undertaken. The results of parametric investigation indicate that the parameter with the strongest influence on inelastic spectra is the slope of the post yield branch. In consideration of that fact, fixed ratios between V_{cr} and V_y and between K_{cr} and K_y were employed. From the experimental results of Paulay and Priestley (1992), Calvi and Pinto (1996), and Pinto (1996), it is reasonable to consider a secant stiffness value at the yield point equal to 50% of the stiffness before V_{cr}. V_{cr} is taken equal to 30% of V_y. The ratio between the cracking and the yielding load influences pinching—a phenomenon that does not occur often for structures with loads higher than approximately 30% of the yielding load V_y. The considered representative slopes of the structural behaviour are:

$K_3 = 0$ (elastic perfect plastic behaviour)
$K_3 = 10\%K_y$ (hardening behaviour)
$K_3 = -20\%K_y$ (softening behaviour)
$K_3 = -30\%K_y$ (softening behaviour)

An axial load equal to 10% of the nominal axial load is assumed. Further details are given in Borzi *et al.* (1999) and Borzi and Elnashai (in press).

4. VALIDATION EXAMPLES

4.1. Response of instrumented buildings to the 1994 Northridge earthquake

On 17 January 1994, an earthquake occurred with an epicentre of about 1 mile south-southwest of Northridge (34°12·53′N; 118°32·44′W; EERI, 1994) and 20 miles west-northwest of Los Angeles. The earthquake had a focal depth of 12 miles with magnitude as shown in Table I.

The main shock was followed by a large number of aftershocks (2000 aftershocks of magnitude larger than 1·5 and 13 aftershocks of magnitude larger than 4 between 18 and 28 January). These occurred in two distinct zones, one of which is associated with the main shock and is outlined by a rectangle extending 10 miles west-northwest from the epicentre of the main shock and about 10 miles to the north-northeast. The second is beneath the Santa Susanna mountains to the northwest (a rectangle 10 by 6 miles).

Four of the instrumented buildings subjected to the 1994 Northridge earthquake are studied herein. Information on these buildings is available on a CD-ROM (J. A. Martin & Associates, 1994). A dynamic procedure of identification was employed in order to evaluate the parameters describing the global behaviour of the buildings. In this way it was possible to define an adequate macro-model to represent the global structural behaviour of each instrumented building. The dynamic identification procedure is based on the evaluation of the fundamental period of vibration of the building considering transfer functions between the ground floor and the levels at which the sensors were positioned. As indicated by Housner and Jenning (1982) the vibration period of a building can be evaluated by considering the transfer function between the base and the roof. In the present work it seems more appropriate to consider the transfer function between the base and the centre of the resultant seismic

force. This choice is due to the fact that the seismic behaviour will be studied based on an equivalent single-degree-of-freedom (SDOF) system with a height equal to that of the centre of mass of the building. The position of the centre of seismic force is a function of the equivalent lateral force distribution. It was observed by Calvi (1996) that as long as the structure remains in the elastic range the displacement shape is linear along the height, hence the choice of an inverted triangular distribution of the lateral loads is valid. This distribution is associated with a height of the resultant of seismic forces equal to 2/3 of the building height. For low-rise structures having distributed inelastic response mechanisms with plastic hinges in the beams, the linear deformation shape is maintained. For tall structures, and for soft storey mechanisms, the centre of seismic loads tends to move downwards. Priestley and Calvi (1991) proposed formulae for the evaluation of equivalent heights. The limit distributions that can be assumed are the inverted triangular and the rectangular distributions.

The period, calculated considering the peak value of the transfer function between the base and the centre of mass, is considered as an equivalent elastic period of vibration. This is because the records are influenced by the damage to the structure and the evaluated stiffness is less than that of the building before the earthquake. The initial elastic period T_I, corresponding to the secant stiffness at the yield point, is defined by an expression given in the Uniform Building Code (UBC, 1997):

$$T_I = C_t \, h_{tot}^{3/4} \tag{1}$$

where h_{tot} is the total height of the building in metres, and C_t is assumed equal to 0·0853 for moment resisting steel frames, 0·0731 for moment resisting reinforced concrete and eccentrically braced steel frames, and 0·0488 for all other structures. The coefficients C_t given by the UBC were derived assuming the gross section of reinforced concrete structural elements. In the technical literature a stiffness of about 50% of uncracked stiffness is normally employed. Therefore, the coefficient C_t is herein multiplied by $\sqrt{2}$ for reinforced concrete structures.

If the seismic analysis is carried out representing the building by an HHS model, the period of vibration of the structure is not sufficient to define all the parameters. Assumptions concerning the shape of the primary (push-over) curve and the relationship between axial and nominal axial loads are also necessary. The axial load amounts to 10% of the nominal concentric axial compressive capacity based on ACI 318-89 (American Concrete Institute, 1989), as assumed for the definition of inelastic response spectra. The shape of the primary curve before the yield point is defined considering $V_{cr} = 30\%V_y$ and $K_y = 50\%K_{cr}$ (Figure 2), as assumed for the definition of response spectra in light of experimental tests. By assuming the post-elastic stiffness and knowing the initial elastic period (calculated according to equation (1), as well as the equivalent elastic period (calculated as the ordinate of the peak value of the transfer functions), the ductility factor of the structure may be obtained from the relationship:

$$\mu = \frac{T_E^2(1-\alpha)}{T_I^2 - \alpha T_E^2} \tag{2}$$

where $\mu$is the global displacement ductility of the structure and α is a coefficient that gives the post-elastic slope of the primary curve ($K_3 = \alpha K_y$).

The peaks of displacement recorded at the centres of mass were compared with the inelastic displacement spectral ordinates. If the building is approximated by a single-degree-of-freedom system (SDOF), the design force will be

$$F_{MAX} = WS_A \tag{3}$$

Table 2. General information on the analysed buildings

	Sherman Oaks 13-storey Commercial Bldg	Van Nuys 7-storey Hotel	Los Angeles 17-storey Residential Bldg	Los Angeles 52-storey Office Bldg
Construction Date	1965	1966	1982	1990
Design Date	1964	1965	1980	1988
Number of Stories	15	7	17	57
Number of Stories Below the Ground	2	0	0	5
Number of Sensors	15	16	14	20
Epicentral Distance	9 km	7 km	32 km	31 km
Soil Condition	Alluvium	Alluvium	Rock	Alluvium over sedimentary rock
Foundation System	Concrete piles	Concrete friction piles	Concrete drilled piles	Concrete spread footings
Lateral Resistance System	Shear wall for the two sub-levels and moment resisting frames from ground to roof along the two principal directions	Moment resisting frames along the two principal directions	Shear walls along the two principal directions	Steel moment frames and braced frames along the two principal directions

Figure 3. View of Sherman Oaks 13-storey commercial building

Figure 4. View of Van Nuys 7-Storey hotel

where W is the weight of the building and S_A is the spectral acceleration. In order to judge whether or not the inelastic acceleration spectra adequately quantify the resistance requirements corresponding to a certain earthquake, the base shear force, calculated by means of the recordings, was compared with

Figure 5. View of Los Angeles 17-storey residential building

Figure 6. Los Angeles 52-storey office building

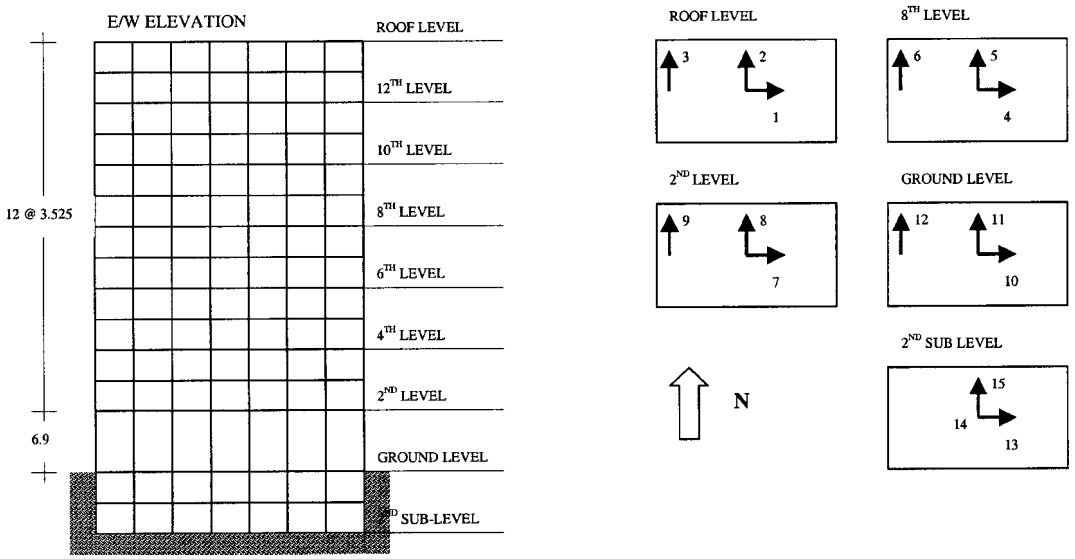

Figure 7. Location of the sensors in the Sherman Oaks 13-storey commercial building

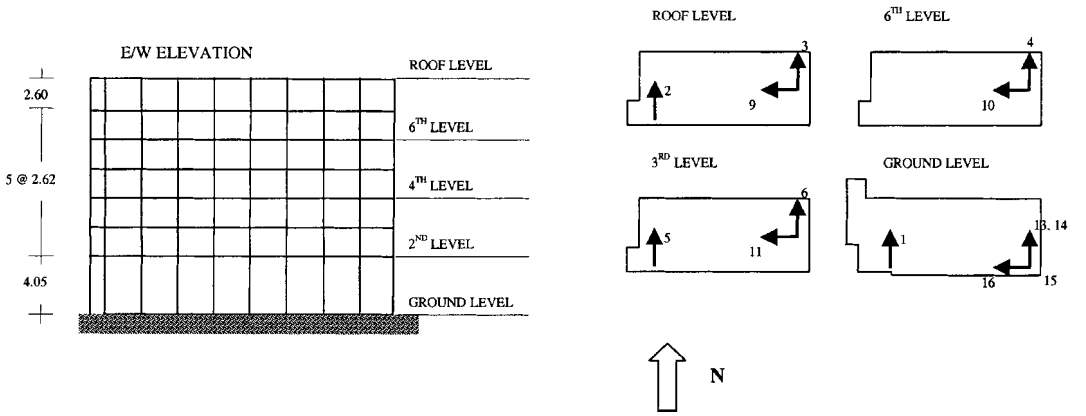

Figure 8. Location of the sensors in the Van Nuys 7-Storey hotel

the inelastic spectral accelerations. To evaluate the base shear, the acceleration was calculated assuming a linear variation between the recorded accelerations in the floors in which the instruments were located. It was assumed that all floors of the MDOF system had the same mass.

4.1·1. Description of the buildings. The global characteristics of the buildings analysed are summarized in Table II. A general view of the buildings is given in Figures 3 to 6, whilst the locations of the sensors are depicted in Figures 7 to 10. For all the buildings of the selected sample, the torsional vibrations are considered negligible.

A large number of cracks were observed in the reinforced concrete components of the lateral system

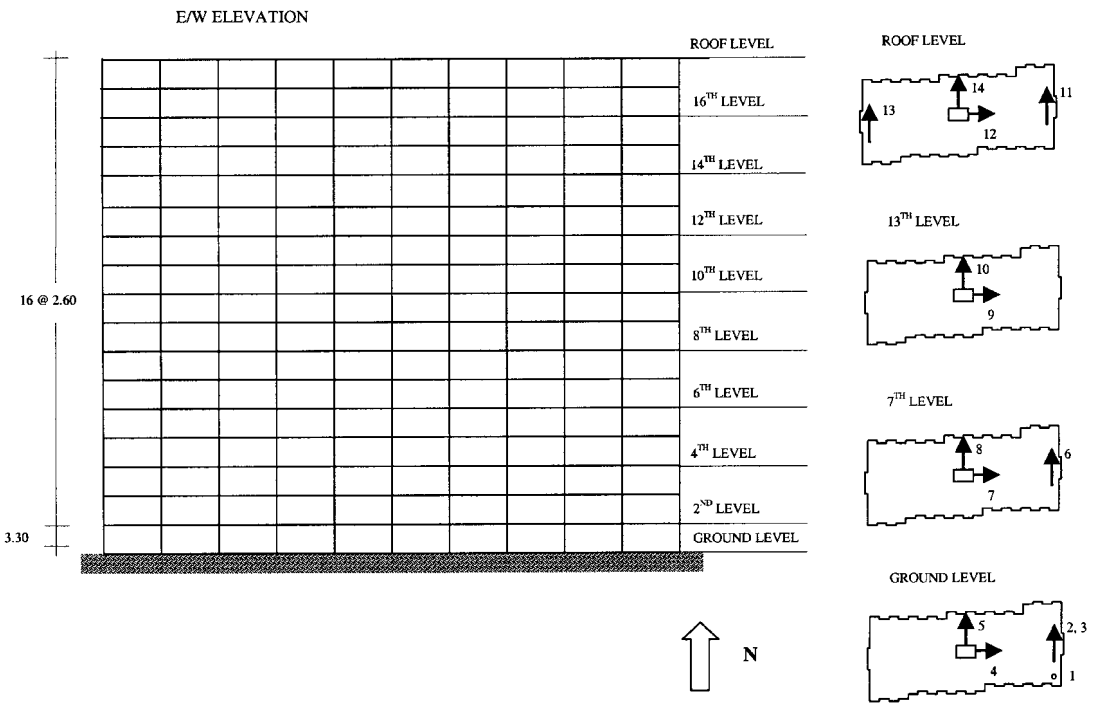

Figure 9. Location of the sensors in the Los Angeles 17-storey residential building

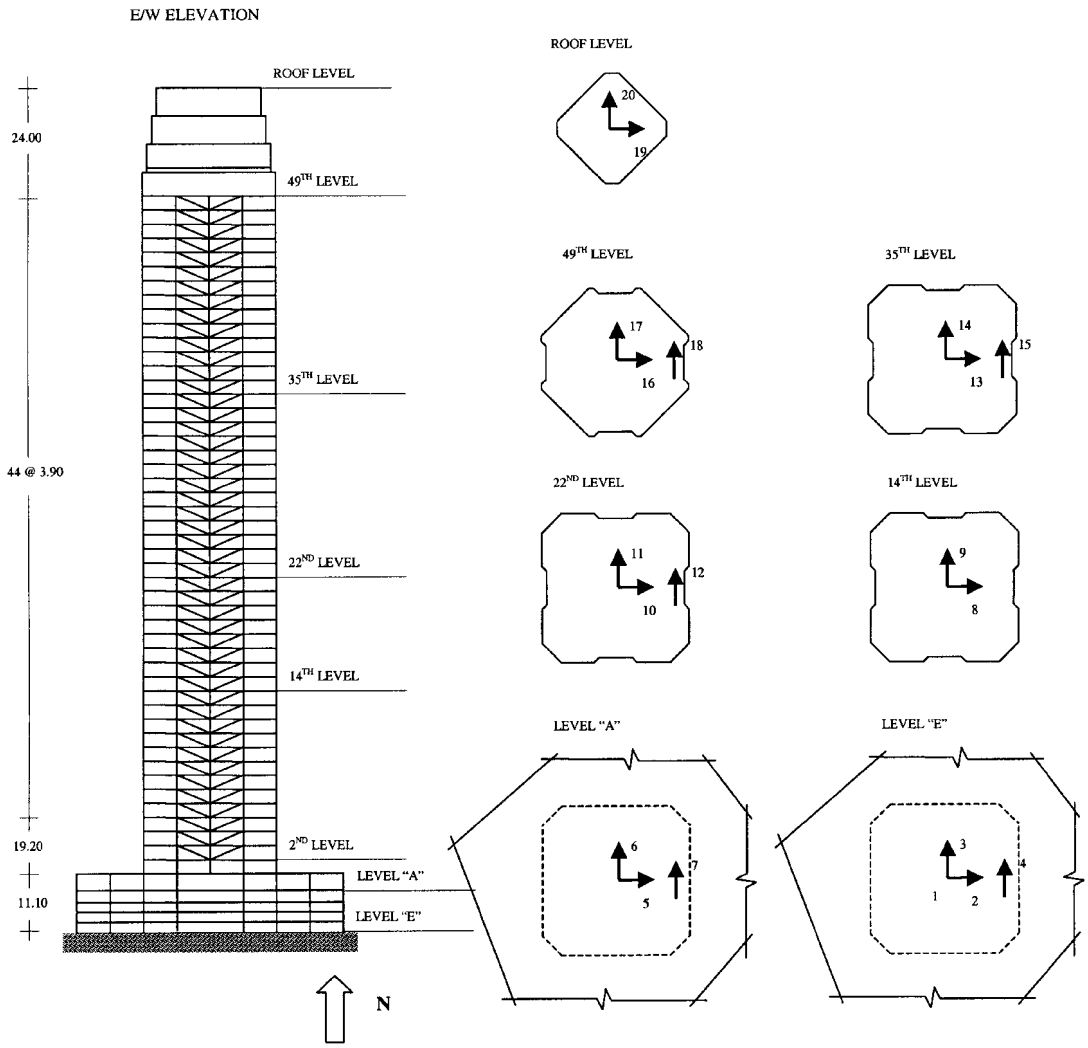

Figure 10. Location of the sensors in Los Angeles 52-storey office building

in the Sherman Oaks 13-storey commercial building making retrofitting necessary. The cracks were repaired by epoxy injection. No significant damage was noticed in the foundations, whilst moderate spalling occurred in columns with light damage in the connections. Non-structural elements suffered light or no damage. The most damaged of the buildings studied was the Van Nuys seven-storey hotel. The moment frame columns on the South face of the fourth floor were seriously damaged owing to shear distress. A permanent lateral tilt of about 40 mm and a vertical set of about 25 mm at the East end of the building were measured. Following the classification of damage given by ATC-13, heavy and moderate damage levels were observed after the earthquake in structural and non-structural elements, respectively. The equipment was only slightly damaged. Both buildings in Los Angeles, the 17-storey residential building and the 52-storey office building, showed very slight damage in their structural and non-structural elements.

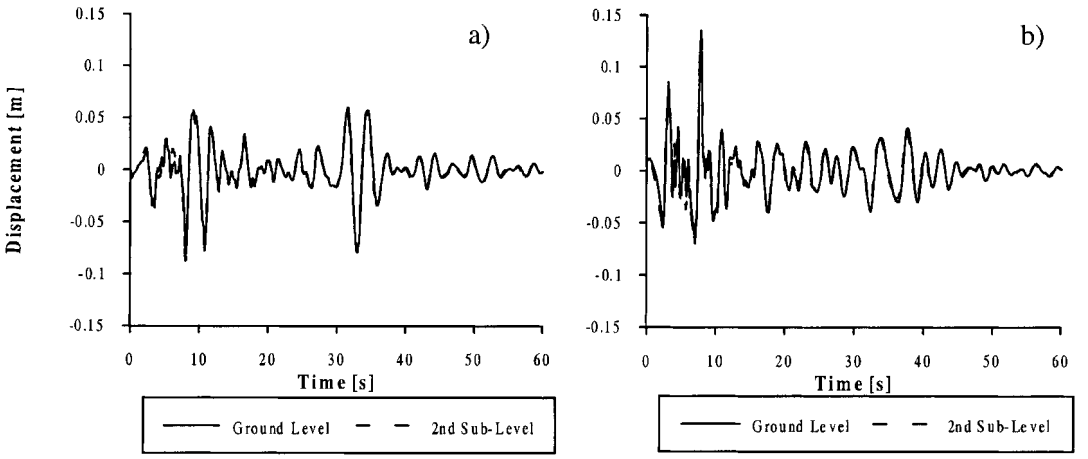

Figure 11. Difference between the recorded motion at the second sub-level and the ground floor in a) east-west and b) north-south directions

4.1·2. Definition of equivalent SDOF systems. The first problem faced in deriving on SDOF system is to determine the extent of the building that should be modelled (including or excluding sub-ground levels). In the Sherman Oaks 13-storey commercial building there are shear walls from the second sub-level to the ground floor, whilst from the ground floor to the roof the lateral load resistance is provided by frames in both directions. The structure is therefore very stiff in the sub-levels and it is reasonable to employ a macro-model only from the ground levels upward. The displacements at the second sub-level and the ground floor are compared to confirm this. The difference between the recorded motion at the second sub-level and the ground floor is negligible for both North–South and East–West directions, as shown in Figure 11. On the other hand, for the Los Angeles 52-storey office building the equivalent SDOF model represents all levels of the building. This is because the sub-ground levels are not as stiff as for the Sherman Oaks 13-storey commercial building.

The records obtained from the closest level to the point of application of the resultant of seismic forces are herein assumed to represent the response of the centre of mass. For the Los Angeles 17-storey residential building only the triangular distribution of lateral loads is studied, because the rectangular distribution does not suit the case of buildings with shear walls (Pauley and Priestley, 1992). For the 52-storey office building an appreciable difference in terms of the position of the resultant force assuming a triangular and rectangular distribution of lateral loads is observed. Therefore, the accelerograms recorded in two different levels are investigated. The assumed positions of the centre of mass are reported in Table III for the building sample considered.

The transfer functions between the accelerograms recorded at the base and at the closest level to the resultant seismic force are shown in Figure 12. By use of frequency domain analyses it is possible to

Table 3. Buildings centre of mass position

Sherman Oaks 13-storey Commercial Bldg	Van Nuys 7-storey Hotel	Los Angeles 17-storey Residential Bldg	Los Angeles 52-storey Office Bldg
8^{TH} level	6^{TH} level	13^{TH} level	22^{ND} and 35^{Th} levels

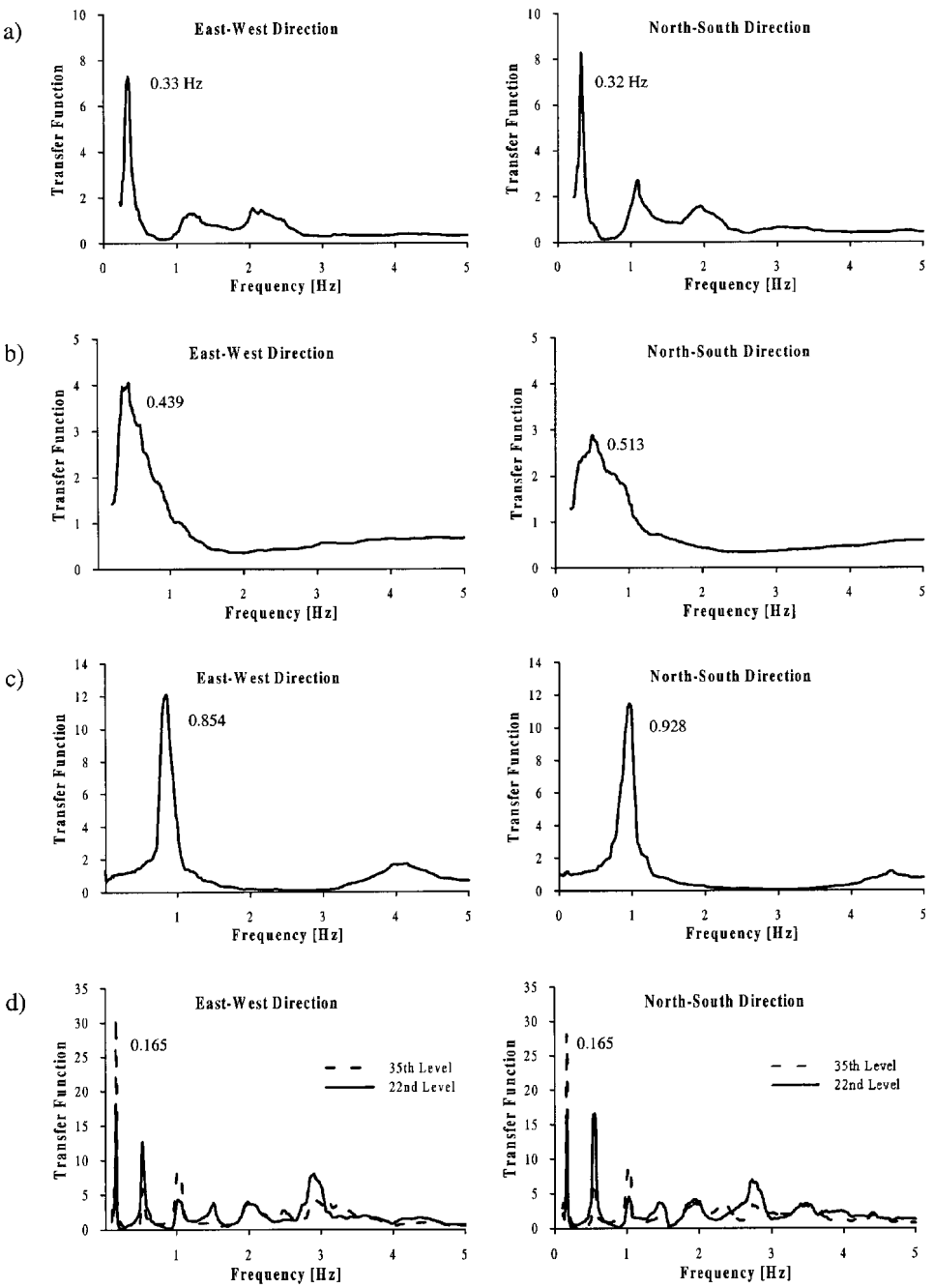

Figure 12. Transfer function between the base and the centre of seismic force of the a) Sherman Oaks 13-storey commercial building, b) Van Nuys 7-storey hotel, c) Los Angeles 17-storey residential buildings and d) Los Angeles 52-storey office building

estimate the fundamental vibration period along both principal directions. These periods of vibration, as well as the elastic counterparts, obtained by means of equation (1), are reported in Table IV.

Table 4. Elastic and equivalent elastic vibration periods

	Sherman Oaks 13-storey Commercial Bldg	Van Nuys 7-storey Hotel	Los Angeles 17-storey Residential Bldg	Los Angeles 52-storey Office Bldg
T_I	1·99 sec	0·99 sec	1·23	5·05
T_E (E-W direction)	3·00 sec	2·28 sec	1·17	6·06
T_E (N-S direction)	3·15 sec	1·95 sec	1·08	6·06

For the 17-storey residential building in Los Angeles it is observed that the structures did not yield during the earthquake because the elastic periods are higher than those from frequency analyses. This is attributed to the elastic period expressions representing an average of many different structural system domains. As a consequence, for this building the peak values of the response will be compared with elastic instead of inelastic response spectra.

For the buildings that exhibited inelastic behaviour, two different assumptions regarding the post-elastic stiffness were made. Elastic-perfectly plastic behaviour as well as hardening were assumed. For the seven-storey hotel, the hardening case was not studied, since this building did not perform well and was severely damaged during the earthquake. For the 52-storey office building, the EPP model is also

Table 5. Comparison between maximum recorded (Δ_{MAX}) displacement and the spectral ordinates (S_D) calculated for the accelerograms at the base of the buildings

	Direction	D_{MAX}	Hysteretic Behaviour	μ	S_D	Error
Sherman Oaks 13-storey						
Commercial Bldg.	E-W	0·249 m	HHS, $\alpha = 0$	2·30	0·182 m	27%
HHS, $\alpha = 10\%$	2·68	0·211 m	15%			
N-S	0·180 m	HHS, $\alpha = 0$	2·51	0·178 m	1%	
HHS, $\alpha = 10\%$	3·01	0·174 m	3%			
Van Nuys 7-storey Hotel	E-W	0·209 m	HHS, $\alpha = 0$	5·30	0·216 m	3%
N-S	0·152 m	HHS, $\alpha = 0$	3·88	0·146 m	4%	
Los Angeles 17-storey						
Res. Bldg.	E-W	0·057 m	Elastic	—	0·072 m	26%
N-S	0·060 m	Elastic	—	0·073 m	32%	
Los Angeles 52-storey Off.						
Bldg. Centre of						
Mass 22^{ND}	E-W	0·071 m	HHS, $\alpha = 0$	1·44	0·139 m	96%
HHS, $\alpha = 10\%$	1·51	0·136 m	92%			
EPP	1·44	0·106 m	49%			
N-S	0·058 m	HHS, $\alpha = 0$	1·44	0·044 m	24%	
HHS, $\alpha = 10\%$	1·51	0·038 m	34%			
EPP	1·44	0·056 m	3%			
Los Angeles 52-storey Off.						
Bldg. Centre of						
Mass 35^{ND}	E-W	0·129 m	HHS, $\alpha = 0$	1·44	0·139 m	8%
HHS, $\alpha = 10\%$	1·51	0·136 m	5%			
EPP	1·44	0·106 m	18%			
N-S	0·080 m	HHS, $\alpha = 0$	1·44	0·044 m	45%	
HHS, $\alpha = 10\%$	1·51	0·038 m	53%			
EPP	1·44	0·056 m	30%			

Table 6. Comparison between maximum recorded base shear (F_{MAX}) and the spectral ordinates (S_A) calculated for the accelerograms at the base of the buildings

	Direction	F_{MAX}	Hysteretic Behaviour	μ	S_A	Error
Sherman Oaks 13-storey						
Commercial Bldg.	E-W	0·075 W	HHS, $\alpha = 0$	2·30	0·081 g	8%
HHS, $\alpha = 10\%$	2·68	0·092 g	23%			
N-S	0·155 W	HHS, $\alpha = 0$	2·51	0·073 g	53%	
HHS, $\alpha = 10\%$	3·01	0·071 g	54%			
Van Nuys 7-storey Hotel	E-W	0·169 W	HHS, $\alpha = 0$	5·30	0·167 g	1%
N-S	0·168 W	HHS, $\alpha = 0$	3·88	0·161 g	4%	
Los Angeles 17-storey						
Res. Bldg.	E-W	0·233 W	Elastic	—	0·213 g	8%
N-S	0·283 W	Elastic	—	0·273 g	3%	
Los Angeles 52-storey						
Office Bldg.	E-W	0·037 W	HHS, $\alpha = 0$	1·44	0·015 g	59%
HHS, $\alpha = 10\%$	1·51	0·015 g	59%			
EPP	1·44	0·012 g	68%			
N-S	0·045 W	HHS, $\alpha = 0$	1·44	0·005 g	89%	
HHS, $\alpha = 10\%$	1·51	0·004 g	91%			
EPP	1·44	0·006 g	87%			

assumed because it is customary for steel buildings to degrade less than reinforced concrete buildings, especially so in that no heavy damage was observed.

4.1·3. Comparison between inelastic spectra and recorded response. The peaks of recorded response are herein compared with the inelastic spectra evaluated for the accelerograms captured at the base as well as with average spectra proposed by Borzi *et al.* (1999) for displacements and Borzi and Elnashai (in press) for accelerations. The average values of response modification coefficients proposed in the aforementioned work were used to obtain the inelastic spectra corresponding to the elastic ones calculated for the pertinent magnitude, distances and soil condition.

Tables V and VI report the comparison between the spectral ordinates calculated for the accelerograms at the base and the recorded peak response of the buildings. Similar comparisons are also shown in Figures 13 and 14 for displacements and accelerations, respectively. From the analysis of the obtained results, it is observed that the HHS model for the case of $K_3 = 0$ gives an adequate description of the global structural behaviour of reinforced concrete buildings. This may be due to the fact that usually for seismic loads the primary curve (which for a model not accounting for degradation in resistance corresponds to the monotonic curve) is reached in few loading and reloading cycles. Therefore the post-elastic stiffness is not an important parameter as far as global cyclic behaviour is concerned. The shape of the primary curve before the yield point (defined by the ratio of V_{cr} to V_y and K_{cr} to K_y as adopted for the definition of average inelastic response spectra in Borzi and Elnashai, in press and Borzi *et al.*, 1999) lead to satisfactory results in terms of the description of the global behaviour of real buildings. For the 52-storey office building, the inelastic displacement ordinates are a good estimate of the peak of displacement recorded in the East–West direction at the 35th level. On the other hand, for the North–South direction the resultant seismic force seems to move downwards to the 22nd floor. This may be due to a different deformed shape associated with vibration along the two principal directions. The results obtained for the aforementioned building also show that, for steel structures that performed well, the degradation of stiffness need not be considered. Therefore, in order

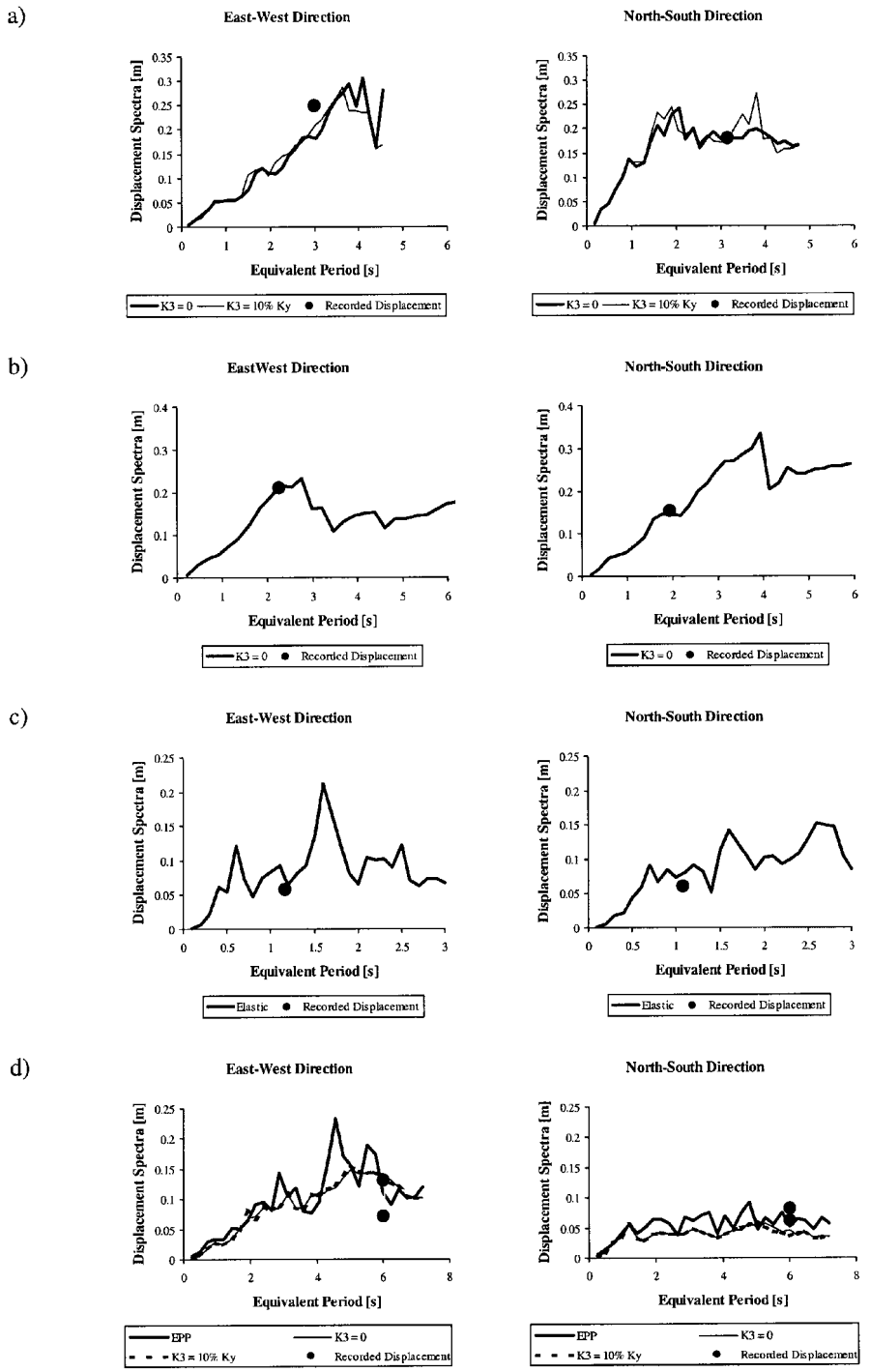

Figure 13. Comparison between maximum recorded displacements and inelastic displacement spectra calculated for the accelerograms at the base for the a) Sherman Oaks 13-storey commercial buildings, b) Van Nuys 7-storey hotel, c) Los Angeles 17-storey residential building and d) Los Angeles 52-storey office building

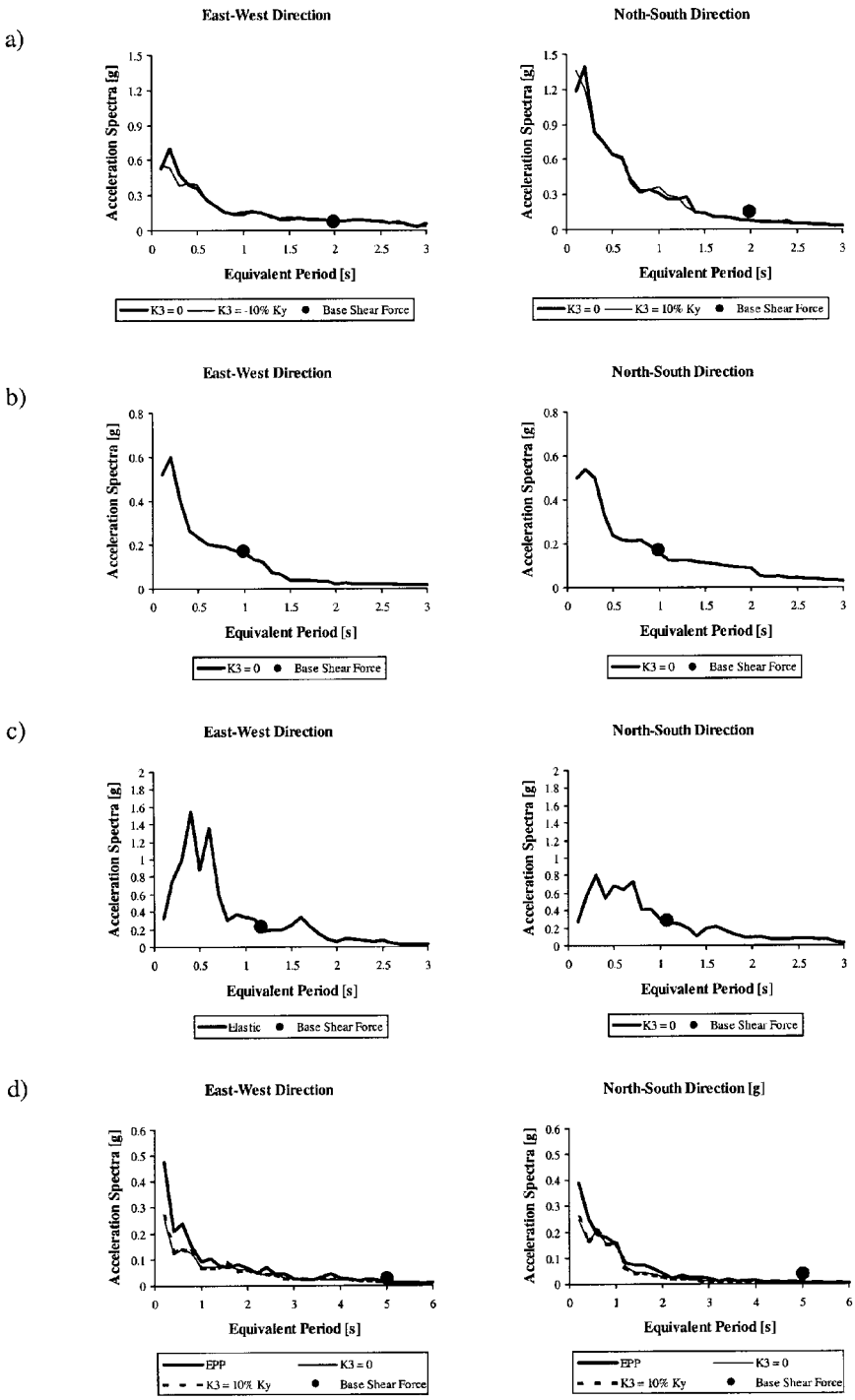

Figure 14. Comparison between maximum shear forces and inelastic acceleration spectra calculated for the accelerograms at the base for the a) Sherman Oaks 13-storey commercial buildings, b) Van Nuys 7-storey hotel, c) Los Angeles 17-storey residential building and d) Los Angeles 52-storey office building

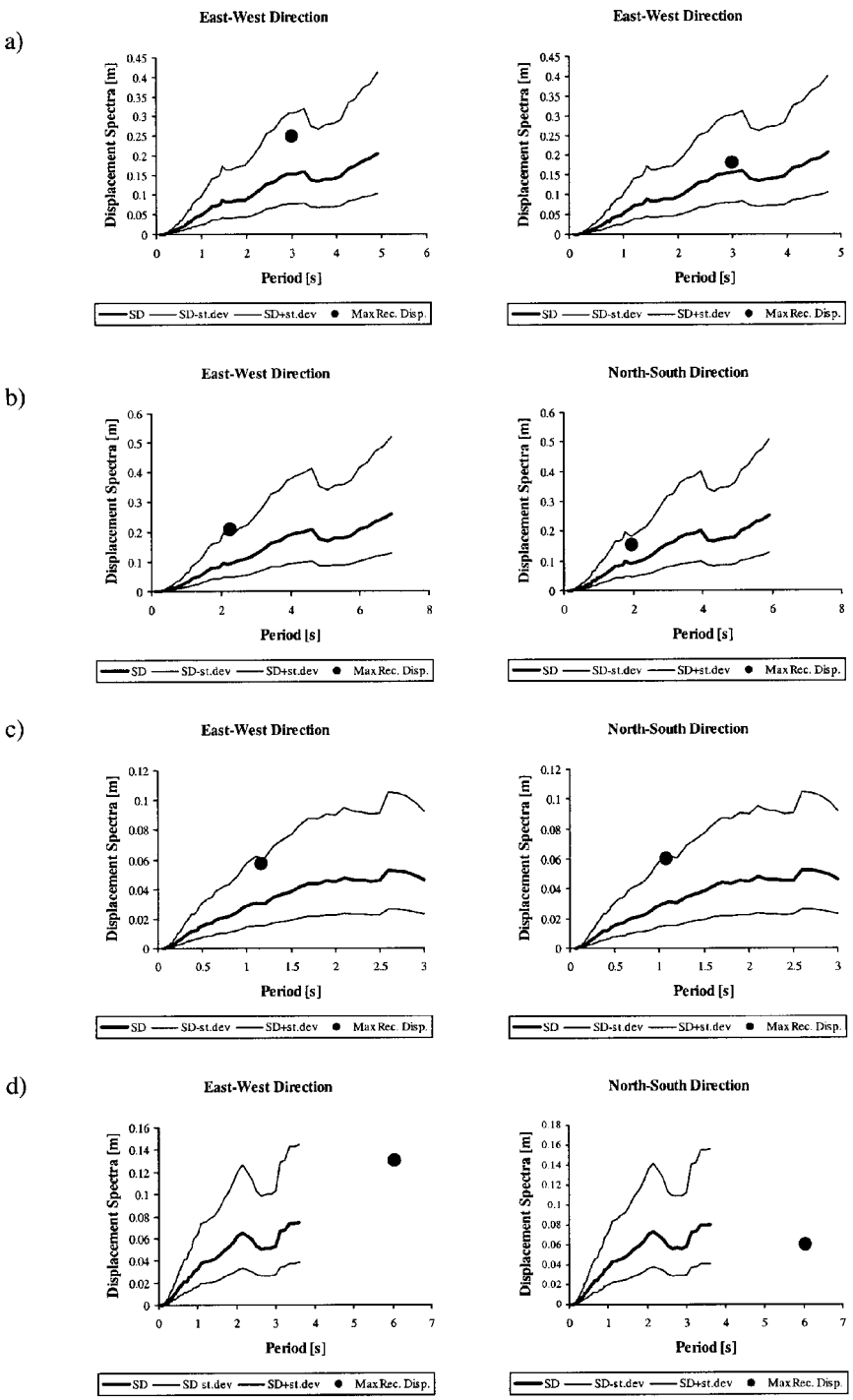

Figure 15. Comparison between average inelastic displacement spectra and maximum recorded displacements in a) Sherman Oaks 13-storey commercial buildings, b) Van Nuys 7-storey hotel, c) Los Angeles 17-storey residential buildings and d) Los Angeles 52-storey office building

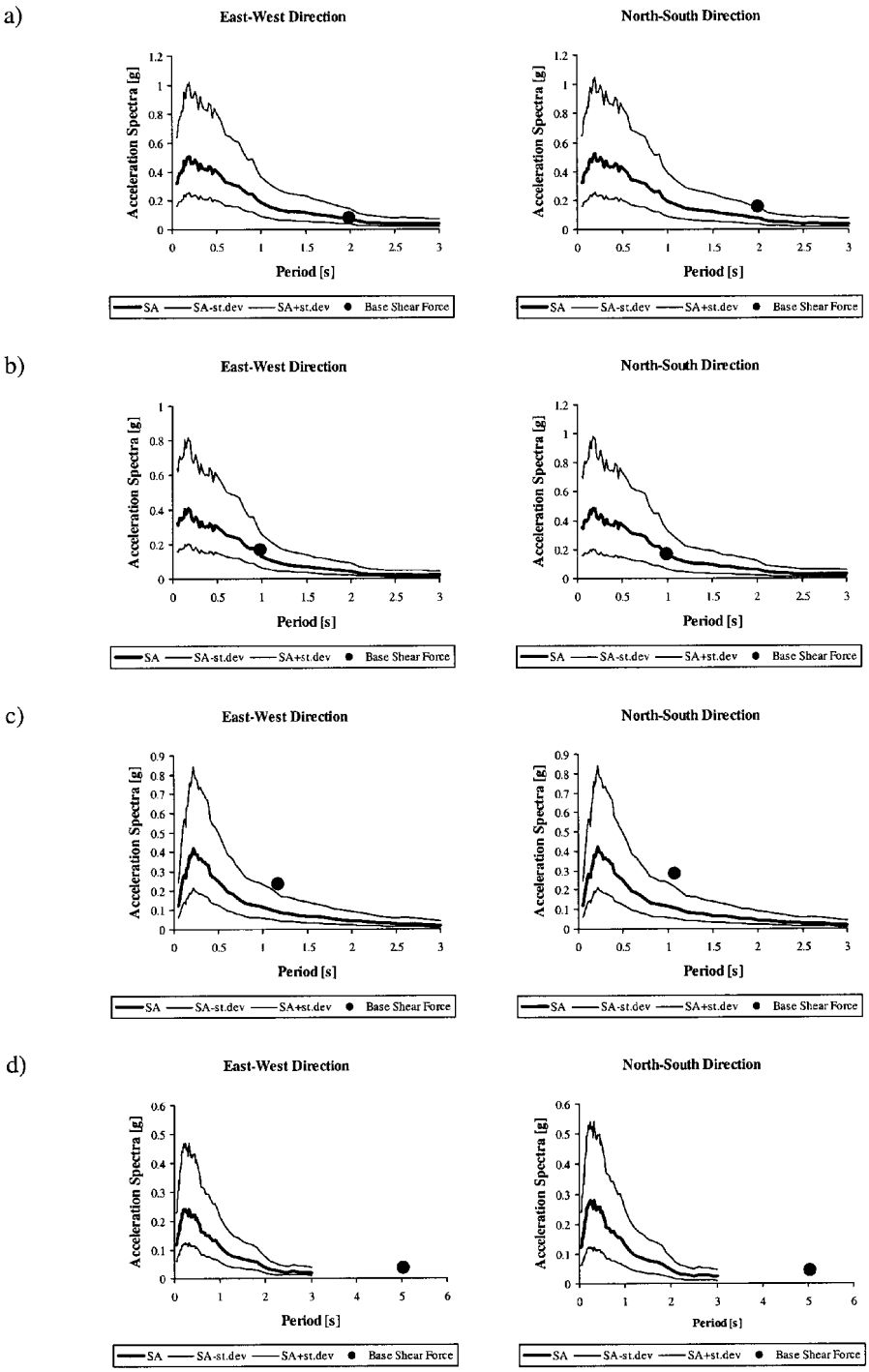

Figure 16. Comparison between average inelastic acceleration spectra and maximum recorded shear forces in a) Sherman Oaks 13-storey commercial buildings, b) Van Nuys 7-storey hotel, c) Los Angeles 17-storey residential building and d) Los Angeles 52-storey office building

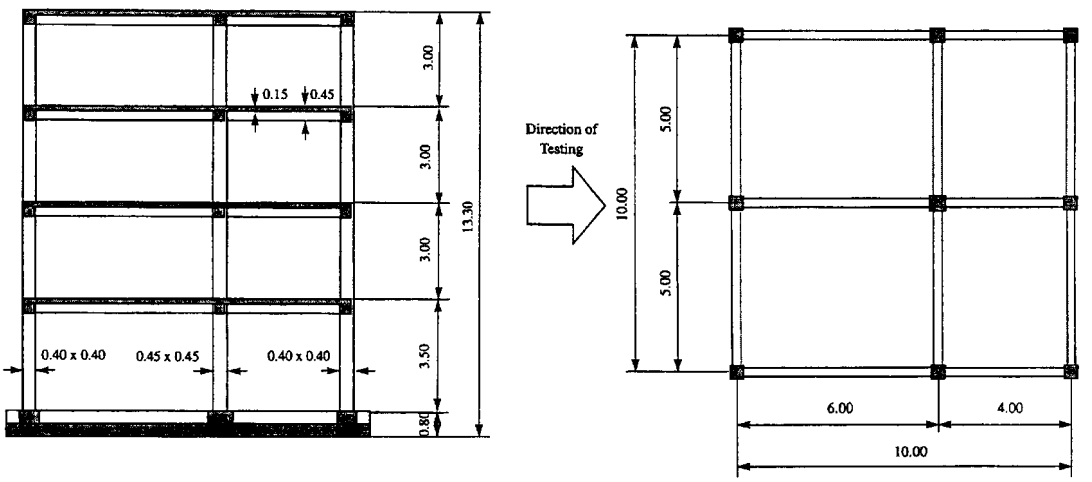

Figure 17. Geometric characteristics of the tested 4-storey full-scale RC building

to describe the global hysteretic behaviour, the EPP model, which is the simplest inelastic force–displacement relationship, is adequate. In some cases the errors in terms of acceleration are large. However, this occurred for buildings that showed a long period of vibration.

The average spectra evaluated in Borzi *et al.* (1999) and Borzi and Elnashai (in press) are also compared with the recorded peak response values. Based on the above observations, the average spectra correspond to the macro-model that gives the best estimate of the peak recorded response. This is shown in Figures 15 and 16 for the displacement and acceleration spectra, respectively. From the aforementioned figures it is observed that the peak response is close to the range of the mean plus or minus one standard deviation for most of the cases considered. The only case in which the spectral ordinates do not adequately represent the response of the building is that of the North–South direction for the Sherman Oaks 13-storey structure. This may be due to the contribution of higher vibration modes that are not taken into account in this approach. In this case, an approach based on acceleration can heavily underestimate the level of force that the building would be subjected to.

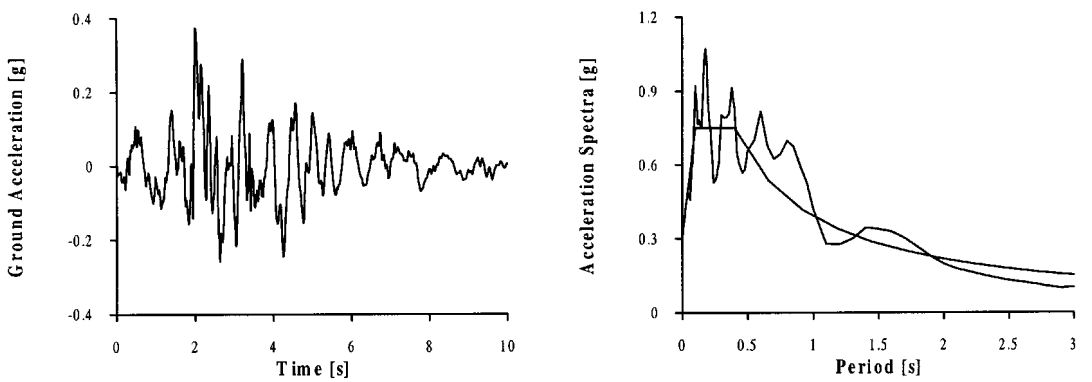

Figure 18. a) Assumed ground acceleration and b) comparison between the elastic acceleration spectrum of the utilized accelerogram and EC8 acceleration spectrum (= 5%) for the test on 4-storey full-scale RC building

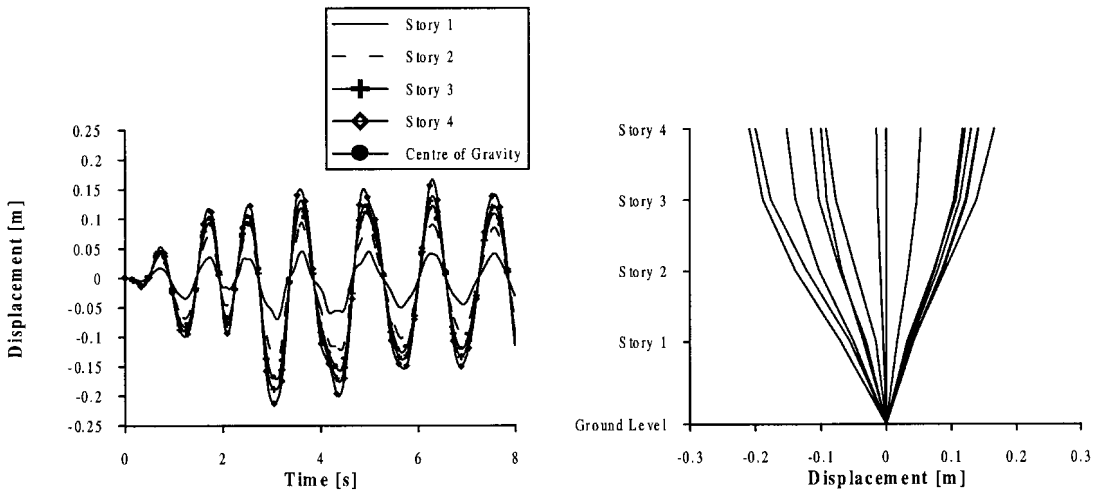

Figure 19. a) Displacement time histories and b) dipslacement profiles at the maximum values of top-storey displacement for the test on the 4-storey full-scale RC building

4.2. Tests on a four-storey full-scale RC building

The results of pseudo-dynamic tests on a four-storey full-scale RC building constructed at the ELSA laboratory (JRC, Ispra) are assessed herein. Test results are included in the validation procedure because more information on the structural behaviour is available for buildings tested under controlled conditions. It was therefore possible to define the parameters of the SDOF models used to study the seismic behaviour of the real structure with a higer degree of exactitude.

The structure is shown in Figure 17. It was designed according to Eurocode 8 (EC8) as a ductility-class 'high' frame, for 0·3*g* peak ground acceleration and medium soil condition (Eurocode 8, 1994). Dimensions in plan are 10 m × 10 m and storey heights are 3 m, except for the ground floor, which is 3·5 m. The structure is symmetric in the testing direction, with two equal spans of 5 m, whilst the other direction is slightly irregular due to different span lengths (6 and 4 m). All columns have square cross sections of 0·4 m sides except for the interior columns, which are 0·45 × 0·45 m. All beams have rectangular cross sections, with a total depth of 0·45 m and a width of 0·3 m. A solid slab of thickness 0·15 m is employed. The materials used were normal-weight concrete C25/30, B500 tempcore rebars and welded mesh.

An accelerogram artificially generated using the waveforms derived from a real signal (the 1976 Friuli earthquake recorded at Tolmezzo), to approximate the EC8 spectrum for a PGA of 0·3*g* was reproduced in the pseudo-dynamic test. The accelerogram and the corresponding acceleration response spectrum are presented in Figure 18.

4.2·1. Model testing. The average value of the damping ratio was about = 1·8%. By means of direct measurements of stiffness performed by displacing one storey at a time and keeping the others fixed, a fundamental frequency of 1·78 Hz was calculated. The mass and stiffness matrices and solution of the eigenproblem are reported in equation (A1 to A3) of Appendix A. The signal amplitude to be used was fixed at 1·5 times the amplitude of the reference signal, corresponding to a peak design acceleration of 0·3*g*. A preliminary test with a scaling factor of 0·4 was also performed. This amplitude was chosen because it represents the serviceability limit-state. Inspection of the model after the test confirmed that no cracking was imposed. The PGA employed

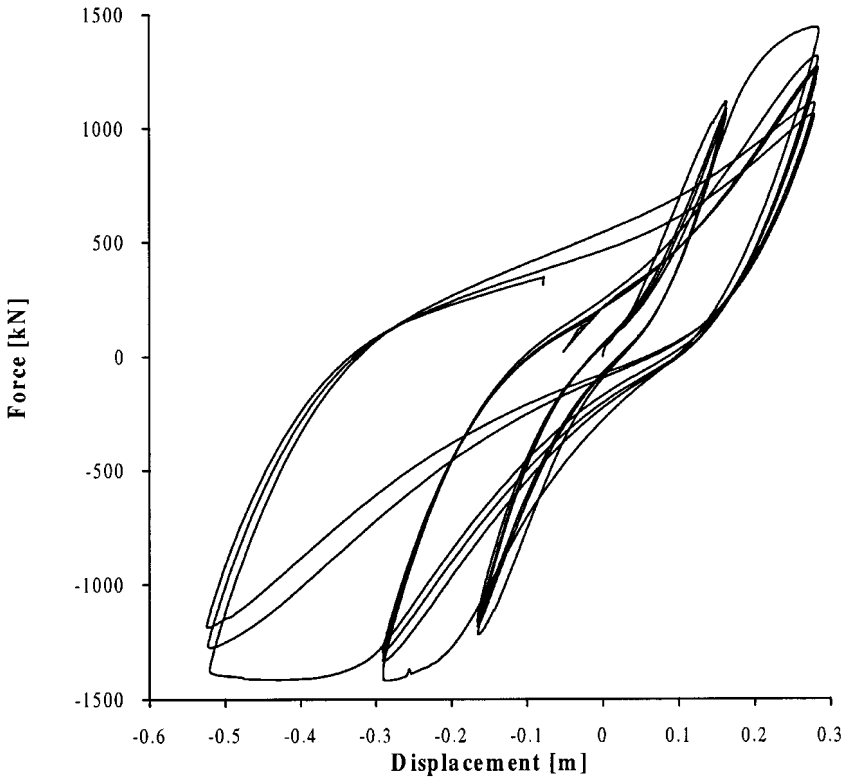

Figure 20. Force-displacement curve for the gravity centre of the 4-storey full-scale RC building recorded during the cyclic test

in the high level test was thought to be representative of the maximum seismic action for which the structure was designed. The structure performed very well; the cracks opened and closed in most critical regions of beams and columns. Only the cracks at the beam–column interface remained permanently opened. A new stiffness measurement was performed immediately after the test. The new stiffness matrix and eigenvalues are reported in equations (A4) and (A5) of Appendix A. After the repair of the structure a final cyclic test was performed. The objective was to impose large inelastic deformations. A damage state considered to be beyond repair resulted. The test results are reported in detail in Negro *et al.* (1994, 1996).

The results of the preliminary stiffness test, low level test and cyclic test were used in the current study to define the SDOF system that gives the best interpretation of the global seismic behaviour of the tested structure. The maximum displacement and shear force achieved in the high level test were then compared with the inelastic spectra calculated for the accelerogram reproduced during the pseudo-dynamic test. The employed average spectra are calculated for input motion parameters such as magnitude and epicentral distance corresponding to the PGA level used in the test.

4.2·2. Definition of equivalent SDOF systems. In order to establish the fundamental vibration mode of the building, the time-history of storey displacement recorded during the high level test and the displacement profiles at the maximum values of top-storey displacement are studied as shown in Figure 19. The latter figure shows that the displacement shape of the structure follows the first modal shape. Thus, it seems reasonable to define an SDOF system representative of the

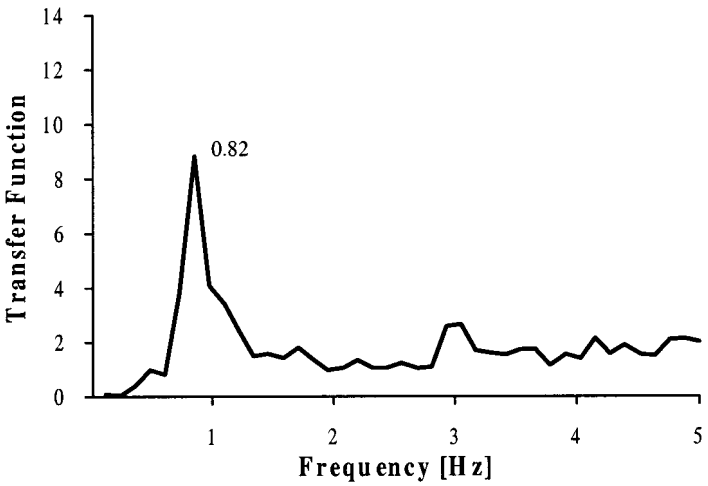

Figure 21. Transfer function between the base and the gravity centre of the 4-storey full-scale RC building

fundamental mode. To confirm this, the mass associated with the first vibration mode was calculated as explained in Appendix A, giving 86% of the total mass corresponding to the fundamental modal mass. The equivalent height of the buildings is evaluated as reported in Appendix A. An average value of $0{\cdot}678h_{\text{tot}}$ is obtained.

From the force–displacement curve of the building centre of mass (positioned at $\frac{2}{3}$ of the height) during the cyclic test (Figure 20) it is confirmed that a V_{cr} equal to 30% V_{y} is adequate to describe the response, as assumed for the definition of inelastic response spectra. Figure 20 also shows that the elastic-perfectly plastic condition is a reasonable representation of the global behaviour of the building, as the envelope under cyclic loads has an almost constant branch in the post-elastic range.

The period of vibration before the cracking load can be obtained from the fundamental frequency f_1 calculated from the initial stiffness test. In this test the displacements imposed on the structure are very small; hence a near elastic stiffness is obtained. This gives a pre-cracked period T_{cr} of 0·562 s.

To define the initial elastic period of vibration, which is the period corresponding to the secant stiffness at the yield point, it is assumed that the secant stiffness is 40–60% of the stiffness before V_{cr} (Paulay and Priestley, 1992). T_{I} is proportional to $K_{\text{y}}{}^{-2}$, hence

$$T_{\text{I}} = \sqrt{\frac{1}{0{\cdot}40}}T_{\text{cr}} = 0{\cdot}889\text{s} \quad \text{to} \quad T_{\text{I}} = \sqrt{\frac{1}{0{\cdot}60}}T_{\text{cr}} = 0{\cdot}725\text{s} \tag{4}$$

These assumptions are supported by the peak values observed in the transfer functions calculated between the base and the storeys for the low level of acceleration in the pseudo-dynamic test. In this case, the period of the first mode is $T_1 = 0{\cdot}746$ s which is between the two values given by equations (4).

To define the required ductility, the equivalent elastic period of vibration is needed. The latter period corresponds to the fundamental frequency f_1 calculated with the stiffness matrix measured after the high level test, i.e. T_{E} is 1·220 s.

The transfer function between the base and the centre of gravity of the building for the high level test is employed to verify the calculated periods, as depicted in Figure 21. The fundamental vibration mode

Table 7. Comparison between recorded and calculated maximum displacements and accelerations during the high level test on the 4-storey full-scale RC building

Recorded Relative Maximum Displacement: 0·172 m					
Calculated Maximum Shear Force: 0·378 W					
T_I	μ	Spectral Displacement	Error in Displacement	Spectral Acceleration	Error in Acceleration
0·889	1·88	0·167 m	3%	0·389 g	3%
0·725	2·83	0·154 m	10%	0·429 g	13%

has a measured frequency of 0·82 Hz, as obtained in the eingenvalue solution. The required ductility is therefore

$$\mu = \frac{T_E^2}{T_I^2} = \begin{cases} 1{\cdot}88 & \text{if } T_I = 0{\cdot}889\text{s} \\ 2{\cdot}83 & \text{if } T_I = 0{\cdot}725\text{s} \end{cases} \tag{5}$$

Finally, in order to evaluate the ratio between axial and nominal axial loads for the HHS model, the ratio between total weight and area of the columns was compared with the compressive resistance of concrete. A ratio of axial to nominal axial load equal to 10% was obtained, making the use of the spectra by Borzi *et al.* (1999) feasible.

4.2·3. Comparison between inelastic spectra and recorded response. The inelastic spectral ordinates, corresponding to the HHS models defined as explained above, were compared with the recorded maximum displacement of the building centre of mass and the peak base shear force. Comparison with the spectra calculated for the accelerogram at the base of the building is reported in Table VII and Figures 22 and 23, whilst the average spectra are shown in Figure 24. The average spectra given in the latter figure are calculated for a magnitude 7·4 event and a distance from the fault of 10 km. The above values correspond to the PGA used in the pseudo-dynamic test.

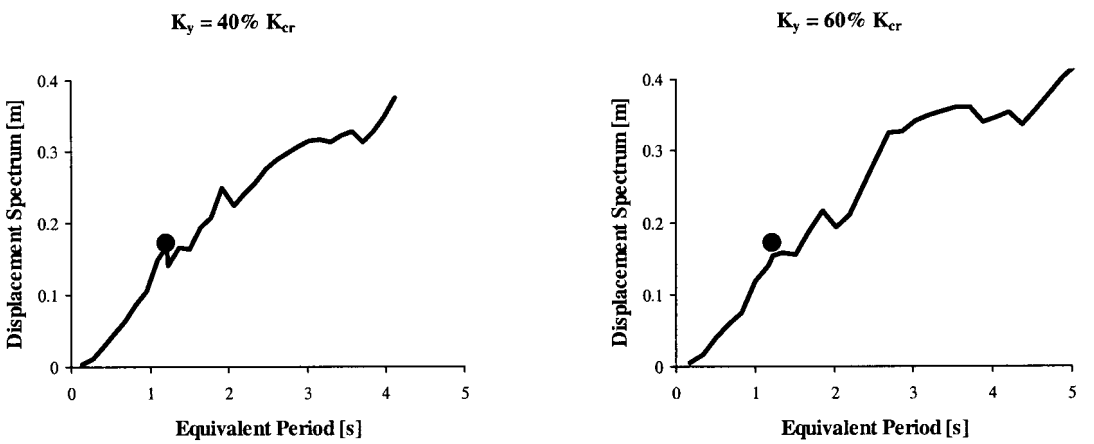

Figure 22. Comparison between inelastic displacement spectra and maximum recorded displacements in the 4-storey full-scale RC building

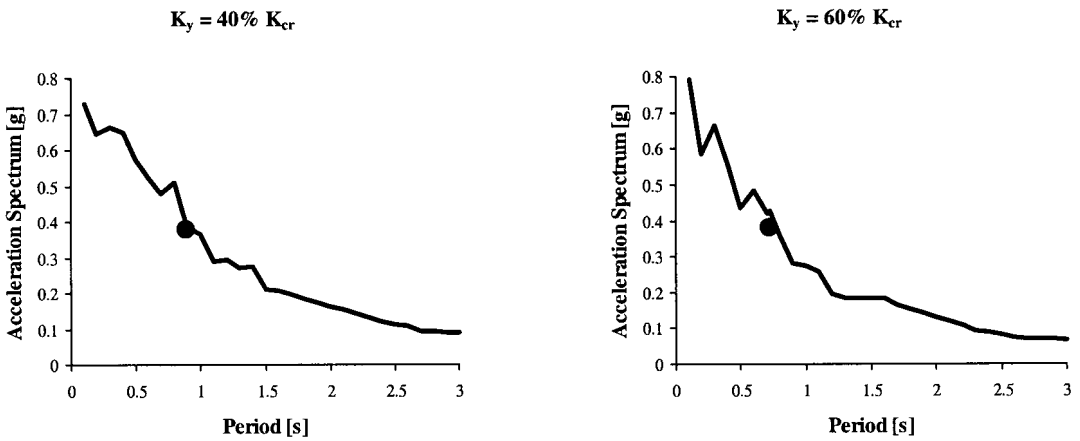

Figure 23. Comparison between inelastic acceleration spectra and maximum base shear force calculated from the records in the 4-storey full-scale RC building

In light of these results, it is confirmed that the inelastic response spectra give a satisfactory estimation of the measured maximum displacement and shear force.

5. CONCLUSIONS

In this paper, an identification procedure has been outlined and applied to real buildings and a full scale test model. The procedure comprises devising an equivalent SDOF system (a substitute structure as defined in Gulkan and Sozen, 1974), the characteristics of which are determined by careful assessment of measured quantities. Once this SDOF system is conceived, it may be used to select appropriate acceleration and/or displacement spectra derived from earthquake databanks (Borzi *et al.*, 1999; Borzi and Elnashai, in press). The acceleration and displacement response of the buildings can therefore be predicted given an earthquake scenario (magnitude and distance) and knowing the site condition.

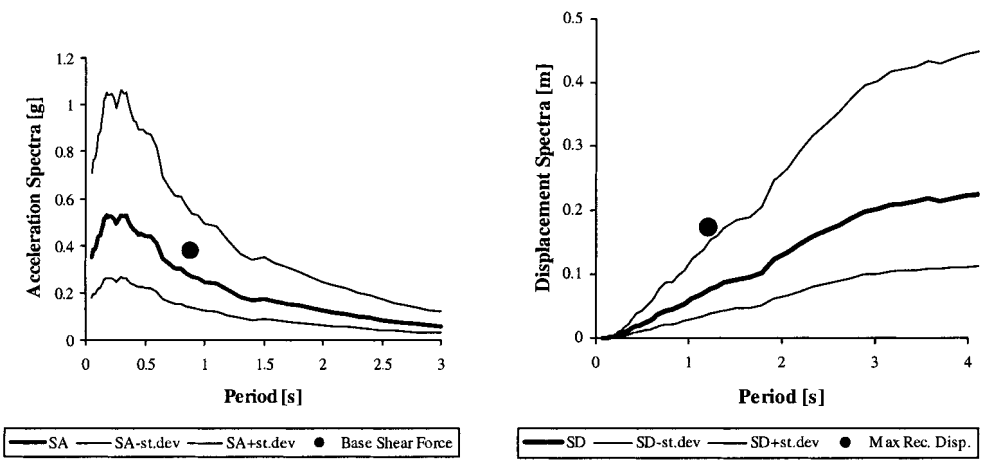

Figure 24. Comparison between average inelastic response spectra and maximum recorded shear forces and displacement

Five application examples are presented in the paper. These comprise four real buildings that were subjected to the Northridge earthquake of 17 January 1994, and a four-storey full-scale 3D pseudo-dynamic test model. The results obtained confirm the following.

- The identification procedure is feasible and easy to apply.
- All assumptions made in the derivation of the substitute SDOF structure are based on mechanics principles and known observations of seismic response.
- The inelastic acceleration and displacement spectra derived in other publications by the authors and their colleagues cover most engineering applications in terms of earthquake characteristics, site condition and structural response parameters.
- In the majority of cases, especially for intermediate period structures, the inelastic spectra, when used alongside the identification procedure outlined in the paper, yield realistic estimates of acceleration and displacement response. They may therefore be used for the assessment of seismic vulnerability.

More work is evidently needed to increase the level of confidence in the methods and tools presented in the paper. However, the results presented for the five buildings are very encouraging.

ACKNOWLEDGEMENTS

The writers would like to express their gratitude to Dr J. J. Bommer (Imperial College, London) and Dr P. Negro (JRC, Ispra) who kindly provided the strong-motion dataset and the test data on the full-scale building, respectively. Special thanks are due to Professor E. Faccioli (Politecnico di Milano) and Professor G. M. Calvi (Universita degli Studi di Pavia) for their constructive suggestions about the necessity of comparing the inelastic spectral ordinates with real building cases. Funding for the support of the primary author at Imperial College was provided by the EU network programs ICONS and NODISASTR.

APPENDIX A

A.1. Mass matrix of the four-storey full scale RC building

$$\boldsymbol{M} = \begin{bmatrix} 86{\cdot}9 & 0 & 0 & 0 \\ 0 & 85{\cdot}9 & 0 & 0 \\ 0 & 0 & 85{\cdot}9 & 0 \\ 0 & 0 & 0 & 83{\cdot}0 \end{bmatrix} \text{ton} \tag{A1}$$

A.2. Stiffness matrix evaluated in the preliminary test and eigenproblem solution

$$\boldsymbol{K} = \begin{bmatrix} 0{\cdot}28328 \times 10^6 & -0{\cdot}16815 \times 10^6 & 0{\cdot}23460 \times 10^5 & -0{\cdot}17750 \times 10^4 \\ -0{\cdot}16480 \times 10^6 & 0{\cdot}25920 \times 10^6 & -0{\cdot}13104 \times 10^6 & 0{\cdot}14620 \times 10^5 \\ 0{\cdot}20990 \times 10^5 & -0{\cdot}13143 \times 10^6 & 0{\cdot}21257 \times 10^6 & -0{\cdot}99870 \times 10^5 \\ -0{\cdot}16000 \times 10^4 & 0{\cdot}13960 \times 10^5 & -0{\cdot}99030 \times 10^5 & 0{\cdot}86611 \times 10^5 \end{bmatrix} \text{kN m}^{-1} \tag{A2}$$

$$\phi = \begin{bmatrix} 0{\cdot}2942 & 0{\cdot}8381 & -0{\cdot}8408 & -0{\cdot}8622 \\ 0{\cdot}5833 & 1{\cdot}0000 & 0{\cdot}0071 & 1{\cdot}0000 \\ 0{\cdot}8399 & 0{\cdot}1280 & 1{\cdot}0000 & -0{\cdot}6209 \\ 1{\cdot}0000 & -0{\cdot}9732 & -0{\cdot}6145 & 0{\cdot}2015 \end{bmatrix} \tag{A3}$$

$$f_1 = 1 \cdot 78\text{Hz}, f_2 = 5 \cdot 12\text{Hz}, f_3 = 8 \cdot 65\text{Hz}; f_4 = 12 \cdot 0\text{Hz}$$

A.3. Stiffness matrix evaluated after the high level acceleration test and eigenproblem solution

$$\boldsymbol{K} = \begin{bmatrix} 0{\cdot}91933 \times 10^5 & -0{\cdot}59704 \times 10^5 & 0{\cdot}13894 \times 10^5 & -0{\cdot}14680 \times 10^4 \\ -0{\cdot}59538 \times 10^5 & 0{\cdot}89812 \times 10^5 & -0{\cdot}53448 \times 10^5 & 0{\cdot}10490 \times 10^5 \\ 0{\cdot}14056 \times 10^5 & -0{\cdot}53020 \times 10^5 & 0{\cdot}85872 \times 10^5 & -0{\cdot}44124 \times 10^5 \\ -0{\cdot}14260 \times 10^4 & 0{\cdot}10263 \times 10^5 & -0{\cdot}44779 \times 10^5 & 0{\cdot}34904 \times 10^5 \end{bmatrix} \text{kN m}^{-1} \tag{A4}$$

$$\phi = \begin{bmatrix} 0{\cdot}2792 & 0{\cdot}8917 & 1{\cdot}0000 & -0{\cdot}7701 \\ 0{\cdot}5984 & 1{\cdot}0000 & -0{\cdot}2517 & 1{\cdot}0000 \\ 0{\cdot}8662 & 0{\cdot}0167 & -0{\cdot}9702 & -0{\cdot}8161 \\ 1{\cdot}0000 & -0{\cdot}8949 & 0{\cdot}7334 & 0{\cdot}3373 \end{bmatrix} \tag{A5}$$

$f_1 = 0{\cdot}82\,\text{Hz},\ f_2 = 2{\cdot}79\,\text{Hz},\ f_3 = 5{\cdot}19\,\text{Hz};\ f_4 = 7{\cdot}34\,\text{Hz}$

A.4. Definition of the mass associated with the first vibration mode

The mass associated with the first vibration mode has been calculated as

$$M^1 = \Gamma_1^2 m_1 \tag{A6}$$

where

$$m_1 = \underline{\phi_1}^{\text{t}} \boldsymbol{M} \underline{\phi_1} \tag{A7}$$

and Γ_1 is the participation factor of the first vibration mode obtained from

$$\Gamma_1 = \frac{\phi_1^{\text{t}} \boldsymbol{M} \boldsymbol{r}}{\phi_1^{\text{t}} \boldsymbol{M} \phi_1} \tag{A8}$$

where r is the unitary vector. The mass associated with the first vibration mode, considering the eigenproblem solution evaluated assuming the stiffness matrix reported in equations (A2) and (A4), is

$$M^1 = 295{\cdot}42 \text{ ton} = 86\% M_{\text{tot}}$$
$$M^1 = 293{\cdot}66 \text{ ton} = 86\% M_{\text{tot}}$$

A.5. Equivalent height of the building

The equivalent height has been calculated as

$$h_e = \frac{\phi_1^t \boldsymbol{Mr}}{r^t \boldsymbol{Mr}} h_{tot} \tag{A9}$$

Therefore, the equivalent height is

$$h_e = 0{\cdot}675 h_{tot}$$
$$h_e = 0{\cdot}683 h_{tot}$$

considering the solution of the eigenproblem evaluated assuming the stiffness matrix reported in equations (A2) and (A4), respectively.

REFERENCES

Ambraseys NN, Simpson KA, Bommer JJ. 1996. Prediction of horizontal response spectra in Europe. *Earthquake Engineering & Structural Dynamics* **25**:371–400.

American Concrete Institute Buildings Code Requirements for Reinforced Concrete 1989. ACI 318-89, American Concrete Institute, Detroid, MI.

Bommer JJ, Elnashai AS, Chlimintzas GO, Lee D. 1998. Review and development of response spectra for displacement-based seismic design. ESEE Research Report N 98-3, ICONS, Imperial College, London.

Bommer JJ, Elnashai AS. 1999. Displacement spectra for seismic design, *Journal of Earthquake Engineering* 1–32.

Borzi B, Calvi GM, Elnashai AS, Faccioli E, Bommer JJ. 1999. Inelastic spectra for displacement-based seismic design. ESEE Research Report No. 99-6, ICONS-NODISASTR, Imperial College. 1999.

Borzi B, Elnashai AS. In press. Refined force reduction factors for seismic design. *Journal of Structural Engineering*.

Calvi GM. 1996. Assessment of Existing Building. CEB Bulletin No. 236; Seismic Design of RC Structures for Controlled Inelastic Response. 159–204.

Calvi GM, Pinto PE. 1996. Experimental and numerical investigations on the seismic response of bridges and recommendations for code provisions. ECOEST & PREC8, Report No. 4.

Eurocode 8, 1994. Design provisions for earthquake resistance of structure 1989. ENV 1998-1, CEN, Brussels.

Gulkan P, Sozen M. 1974. Inelastic response of reinforced concrete structures to earthquake motions. *ACI Journal* **71**:604–610.

Housner G, Jenning P. 1982. Earthquake design criteria. *Monograph*, EERI.

J.A. Martin & Associates. 1994. January 17, 1994, Northridge, California Earthquake. Instrumented Buildings Information System.

Negro P, Pinto AV, Verzelletti G, Magonette GE. 1996. PsD test on four-story R/C building designed according to Eurocodes. *Journal of Structural Engineering, ASCE* **122**:1409–1417.

Negro P, Verzeletti G, Magonette GE, Pinto AV. 1994. tests on a four-storey full-scale R/C frame designed according to Eurocodes 8 and 2: preliminary report. EUR 15879, Ispra (VA), Italy.

Paulay T, Priestley MJN. 1992. *Seismic Design of Reinforced Concrete and Masonry Buildings*. Wiley-Interscience.

Pinto AV. 1996. Pseudodynamic and shaking table tests on RC, bridges. ECOEST & PREC8, Report No. 5.

Priestley MJN, Calvi GM. 1991. Toward a capacity—design assessment procedure for reinforced concrete frame. *Earthquake Spectra* **7**:413–437.

Saatcioglu M, Ozcebe G. 1989. Response of reinforced Concrete Columns to Simulated Seismic Loading. *ACI Structural Journal* 3–12.

Saatcioglu M, Ozcebe G, Lee BCK. 1988. Tests of reinforced concrete columns under uniaxial and biaxial load reversals. Department of Civil Engineering University of Toronto, Toronto, Canada.

UBC (Uniform Building Code), 1997. Structural Engineering Design Provisions. vol **2**.

